Supplementary Information

Characterizing global evolutions of complex systems via intermediate network representations
by Koji Iwayama, Yoshito Hirata, Kohske Takahashi, Katsumi Watanabe,
Kazuyuki Aihara, Hideyuki Suzuki

S1 Numerical Simulations

For the numerical simulations, we used coupled logistic maps on time-evolving networks. We denote the adjacency matrix of the network at time t by $W_{ij}(t)$. When the network is weighted, $W_{ij}(t)$ means the weight between nodes i and j. On the other hand, when the network is unweighted, $W_{ij}(t) = 1$ and $W_{ij}(t) = 0$ indicate the existence and nonexistence of the link between nodes i and j, respectively. The dynamics of the nodes in the time-evolving network is described as follows:

$$\begin{aligned} x_k(t+1) &= f(x_k(t)) + K\sum_l W_{lk}(t) f(x_l(t)), \\ f(x) &= ax(1-x), \end{aligned} \tag{S1}$$

where $x_k(t)$ is the state of the kth node at time t, a is the parameter of the logistic map, and K determines the strength of the interactions between connected nodes. In the following two simulations, we set $a = 3.8$ and $K = 0.004$.

S1.1 Periodically evolving networks

In the first numerical simulation, the weighted network $\boldsymbol{W}(t)$ evolves periodically. The network is described as

$$\begin{aligned} W_{1,2}(t) &= W_{2,1}(t) = 1 + \sin(2\pi t/8000), \\ W_{1,4}(t) &= W_{4,1}(t) = 1 + \sin(2\pi(t+1000)/8000), \\ W_{2,3}(t) &= W_{3,2}(t) = 1 + \sin(2\pi(t+2000)/8000), \\ W_{2,5}(t) &= W_{5,2}(t) = 1 + \sin(2\pi(t+3000)/8000), \\ W_{3,4}(t) &= W_{4,3}(t) = 1 + \sin(2\pi(t+4000)/8000), \end{aligned}$$

$$W_{4,5}(t) = W_{5,4}(t) = 1 + \sin(2\pi(t + 5000)/8000),$$

$$W_{1,5}(t) = W_{5,1}(t) = 1 + \sin(2\pi(t + 6000)/8000).$$

The elements that are not defined here are all 0. Thus, $\boldsymbol{W}(t)$ is symmetric.

We performed the simulation 100 times. The plot of averages and standard deviations of the τ-recurrence rate is shown in Fig. S1. If the time series does not have any periodicity, the number of points plotted at $(i, i + \tau)$ in its recurrence plot is distributed binomially. The red dashed line represents the 5 % significance level of this binomial distribution. The peak values at times 8000 and 16000 are significantly large. Thus, the periodicity of the time-evolving network is correctly extracted.

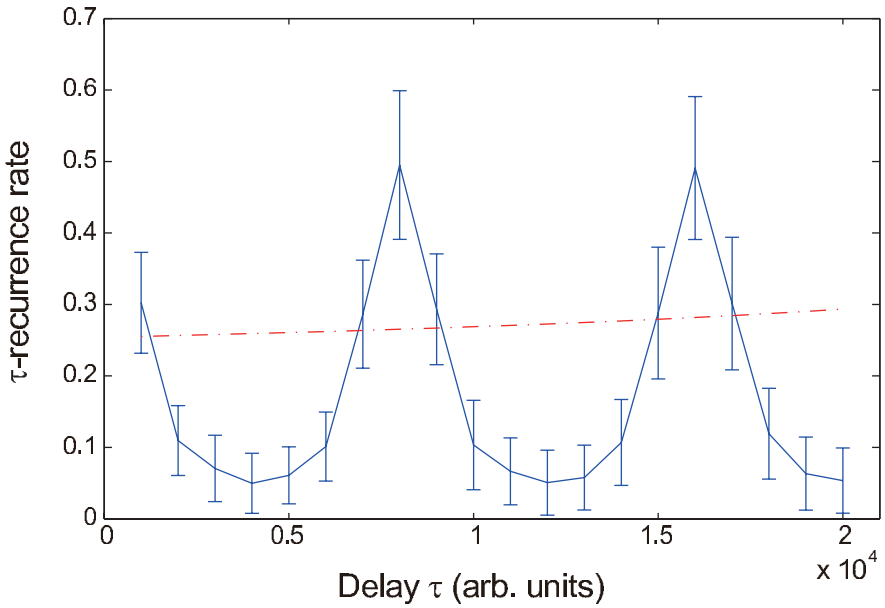

Figure S1: The plot of τ-recurrence rate vs. τ. Error bars indicate standard deviations. The red dash-dotted line shows the 5 % significance level of the null hypothesis that τ-recurrence rates obey the binomial distribution irrespective of τ.

S1.2 Stochastically switching networks

In the second simulation, the network switches stochastically. We prepared five instances of random networks represented by the adjacency matrices $\boldsymbol{W}^n$ $(n = 1, \ldots, 5)$ that consist of ten nodes. Each pair of nodes is connected with the probability 0.4. We set the initial network as $\boldsymbol{W}(1) = \boldsymbol{W}^1$ and switch the network to another instance with

probability 0.0001 at each time step.

We define the true recurrence plot of network patterns as

$$R_{i,j}^{t} = \begin{cases} 1, & \text{if} \quad \boldsymbol{W}(i) = \boldsymbol{W}(j), \\ 0, & \text{otherwise.} \end{cases} \tag{S2}$$

We set the threshold of the long-term global recurrence plot such that the number of points in the long-term global recurrence plot is equal to that of the true recurrence plot. Then, we define the precision of the recurrence plot as the ratio of the number of points in both recurrence plots to the total number of points in the recurrence plot. To validate the effectiveness of the proposed method, we constructed the recurrence plot from the raw time series $\boldsymbol{x}(t)$ instead of the meta-time series. We call it a 'raw recurrence plot.' The three recurrence plots of one realization are shown in Fig. S2.

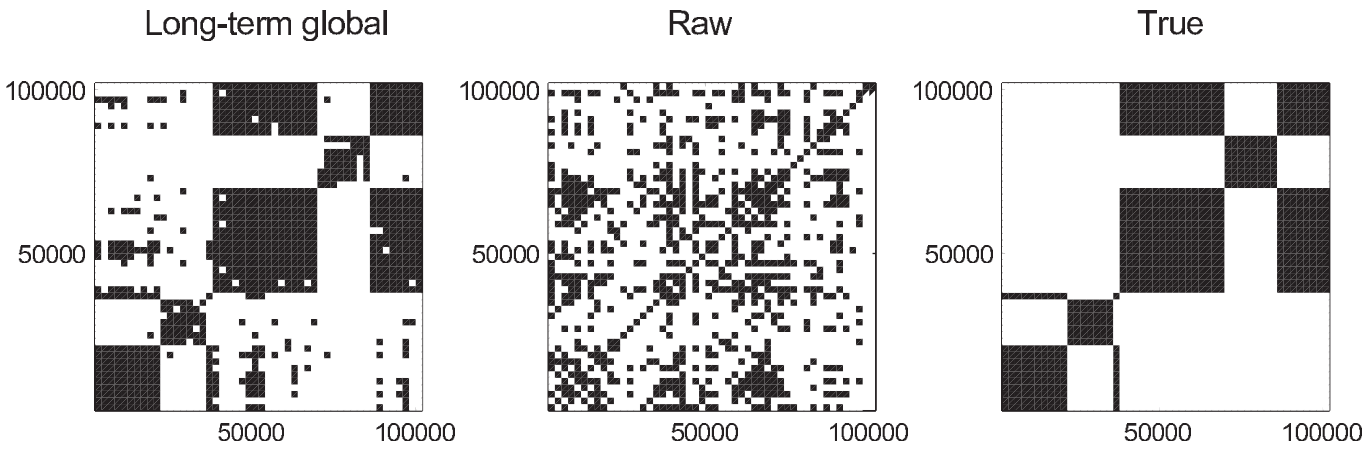

Figure S2: The example of three recurrence plots. The long-term global recurrence plot of the meta-time series (left) is more similar to the true recurrence plot (right) than the raw recurrence plot (centre).

We performed the simulation 100 times. Precisions of long-term global recurrence plots and raw recurrence plots of 100 simulations are shown in Fig. S3. The precision of the long-term global recurrence plots is significantly higher than that of the raw recurrence plots ($p = 3.9 \times 10^{-18}$, Wilcoxon signed-rank test).

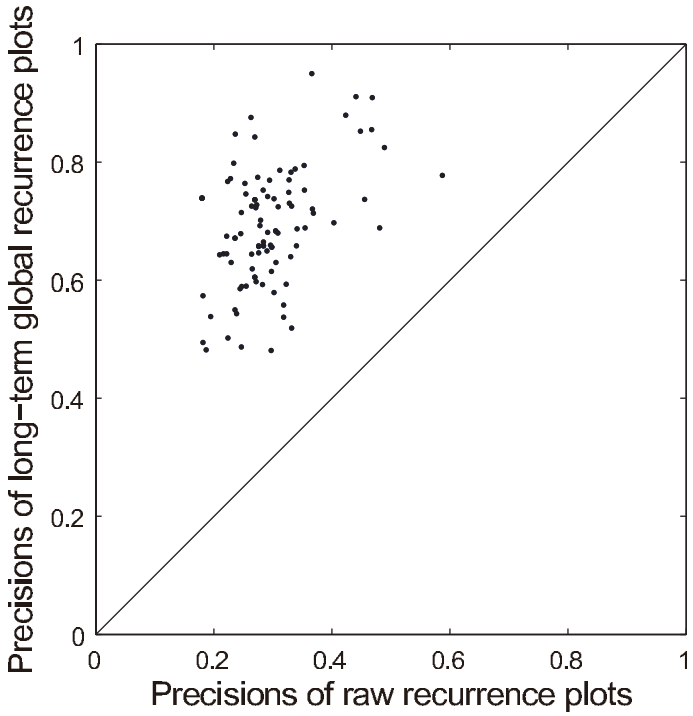

Figure S3: The plot of precisions of long-term recurrence plots against those of raw recurrence rates. Averages and standard deviations of precisions of long-term global and raw recurrence plots are 0.69 ± 0.1 and 0.29 ± 0.07, respectively.

S2 Application of other methods for real data

S2.1 Foreign exchange

For comparison with the proposed method, we analysed the datasets of foreign exchange markets using a combination of conventional methods, namely, the method of Casdagli[1] and the edit distance for marked point processes[2]. We first calculated the edit distance for each pair of currency we used in this study for each pair of times. Second, for each pair of times, we summed up all the edit distances calculated for all the considered pairs to obtain the recurrence plot of the entire foreign exchange market. Third, we obtained a recurrence plot with a threshold such that the recurrence rate became 0.05. Fourth, we coarse-grained the recurrence plot with a window size of 12 to obtain a meta-recurrence plot[1](Fig. S4). Fifth, we finally calculated the τ-recurrence rate for the meta-recurrence plot.

We found that the obtained τ-recurrence rate shows a periodicity of a day; however, the half-a-day periodicity could not be observed (see Fig. S5).

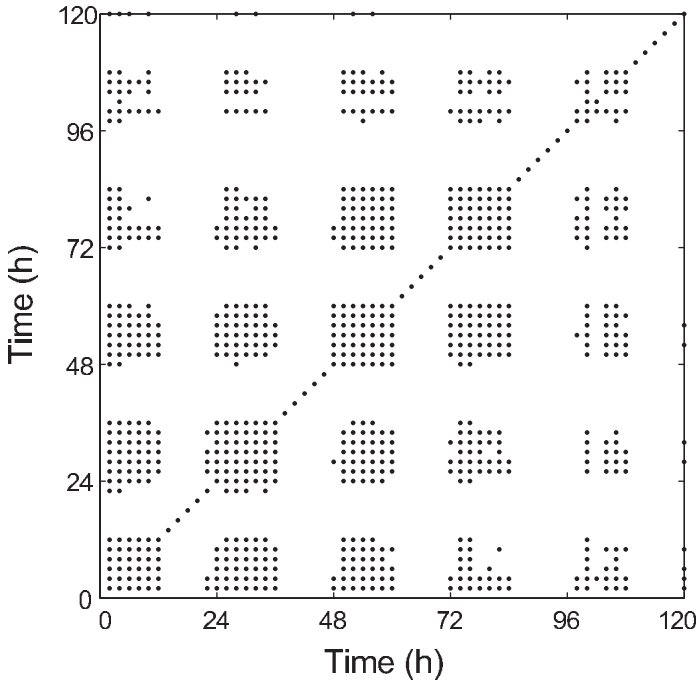

Figure S4: The meta-recurrence plot of foreign exchange markets.

S2.2 Magnetoencephalogrpahy

To validate the effectiveness of the proposed method, we applied an existing method[3] for MEG data and compared the results. We calculated the distributions of numbers of motifs[4] appearing in the meta-time series of networks. Because we considered undirected networks, only two types of motifs are considered: Motif 1, in which one node connects the other two nodes, and Motif 2, in which each of the three nodes is connected to the other two nodes (Fig. S6). The distributions are shown in Fig. S7. The distributions showed no significant difference between the durations within and without 5 s before and after perceptual alternations (motif 1: $p = 0.17$; motif 2: $p = 0.087$, Wilcoxon rank-sum test).

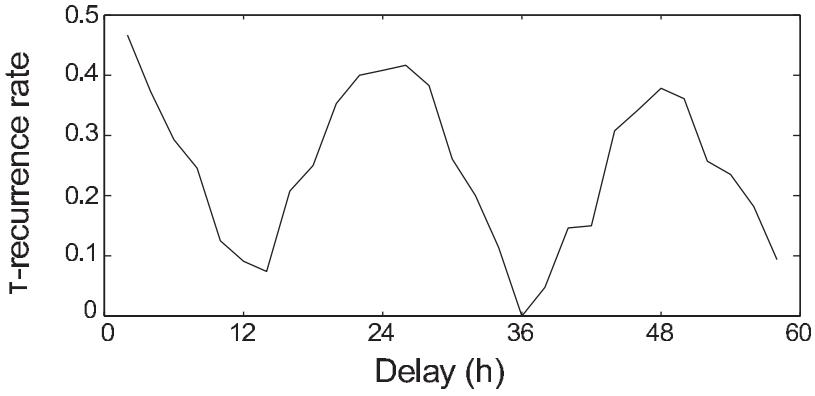

Figure S5: The τ-recurrence rate for the meta-recurrence plot in Fig. S4. The periodicity of a day appears.

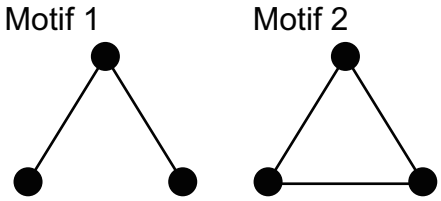

Figure S6: Two types of three-node motifs in undirected networks.

References

[1] Casdagli, M. C. Recurrence plots revisited. *Physica D* **108,** 12-44 (1997).

[2] Suzuki, S., Hirata, Y. & Aihara, K. Definition of distance for marked point process data and its application to recurrence plot-based analysis of exchange tick data of foreign currencies. *Int. J. Bifurcat. Chaos* **20,** 3699-3708 (2010).

[3] de Vico Fallani, F., Latora, V., Astolfi, L., Cincotti, F., Mattia, D., Marciani, M. G., Salinari, S., Colosimo, A. & Babiloni, F. Persistent patterns of interconnection in time-varying cortical networks estimated from high-resolution EEG recordings in humans during a simple motor act. *J. Phys. A: Math. Theor.* **41,** 224014 (2008).

[4] Milo, R., Shen-Orr, S., Itzkovitz, S., Kashtan, N., Chklovskii, D. & Alon, U. Network motifs: simple building blocks of complex networks. *Science* **298,** 824-827 (2002).

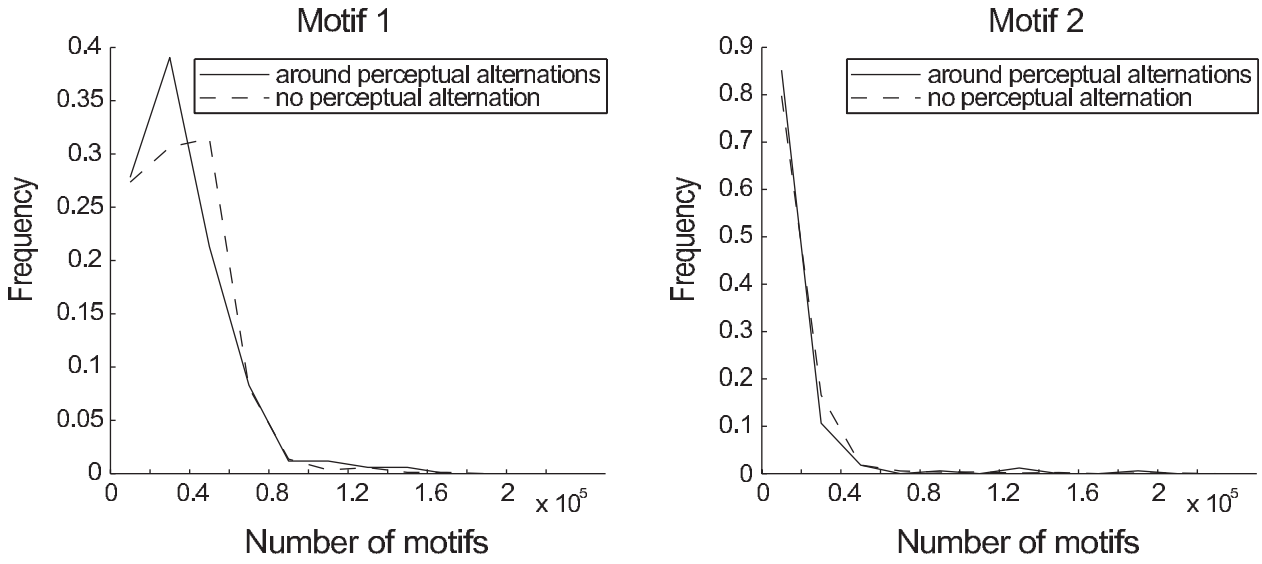

Figure S7: The distributions of the numbers of motifs which appeared within the meta-time series of networks. Solid lines indicate the distributions around perceptual alternations. Dashed lines indicate the distributions while no perceptual alternation was reported.